scientific reports

Check for updates

OPEN

Predicting lateral pelvic lymph node metastasis in rectal cancer patients using MRI radiomics: a multicenter retrospective study

Jeongin Yoo[1,2], Jun Young Han[3], Won Chang[4], Bo Yun Hur[5], Jae Hyun Kim[1,2], Yunhee Choi[6], Soo Jin Kim[7] & Se Hyung Kim[1,2,8]✉

MRI has relatively low sensitivity and specificity in detecting lymph node metastases. This study aimed to develop and validate an MRI radiomics-based model for predicting lateral pelvic lymph node (LPLN) metastasis in rectal cancer patients who underwent LPLN dissection, and to compare its performance with that of radiologists. This multicenter retrospective study included 336 rectal cancer patients (199 men; mean age, 58.9 years ± 11.1 [standard deviation]) who underwent LPLN dissection. Patients were divided into development (*n* = 190) and validation (*n* = 146) cohorts. Radiomics features were extracted from MR images, and the Least Absolute Shrinkage and Selection Operator regression was used to construct radiomics and clinical-radiomics models. Model performance was compared with radiologists using receiver operating characteristic (ROC) analysis. Malignant LPLN was diagnosed in 32.4% of the development cohort (65/190) and 32.9% of the validation cohort (48/146) (*P* = 0.798). Seven radiomics features and two clinical features were selected. The radiomics and clinical-radiomics models demonstrated area under the curves (AUCs) of 0.819 and 0.830 in the development cohort and 0.821 and 0.829 in the validation cohort, respectively. The optimal cut-off (– 0.47) yielded sensitivities of 72.3% and 45.8% and specificities of 82.4% and 87.8% in the development and validation cohorts, respectively. Decision curve analysis indicated no additional net benefit from the clinical-radiomics model compared to the radiomics-only model. Radiologists' AUCs were significantly lower than that of the radiomics model (0.842) and improved with radiomics probability scores (0.734 vs. 0.801; 0.668 vs. 0.791). The MRI-based radiomics model significantly improves the prediction of LPLN metastasis in rectal cancer, outperforming conventional criteria used by radiologists.

Trial registration: Retrospectively registered.

Keywords Rectal neoplasms, Magnetic resonance imaging, Radiomics, Lymphatic metastasis, Lymph node excision

Abbreviations

AUC	Area under the curve
CRT	Chemoradiotherapy
LN	Lymph node
LPLN	Lateral pelvic lymph node
LPLND	Lateral pelvic lymph node dissection
nCRT	Neoadjuvant chemoradiotherapy
ROI	Region of interest
ROC	Receiver operating characteristic

[1]Department of Radiology, Seoul National University Hospital, 101 Daehakro, Jongno-gu, Seoul 03080, Korea. [2]Department of Radiology, Seoul National University College of Medicine, Seoul, Korea. [3]College of Medicine, Seoul National University, Seoul, Korea. [4]Department of Radiology, Seoul National University Bundang Hospital, Seongnam, Korea. [5]Department of Radiology, Healthcare System Gangnam Center, Seoul National University Hospital, Seoul, Korea. [6]Medical Research Collaborating Center, Seoul National University Hospital, Seoul, Korea. [7]Department of Radiology, National Cancer Center, Goyang, Korea. [8]Institute of Radiation Medicine, Seoul National University Medical Research Center, Seoul, Korea. ✉email: shkim71@snu.ac.kr

TME Total mesorectal excision

Rectal cancer ranks as the 8th most common cancer globally, posing significant health challenges[1]. The adoption of total mesorectal excision (TME) since the late 1980s has significantly reduced local recurrence rates[2–4]. However, TME does not address metastasis to lateral pelvic lymph nodes (LPLNs), common in low and mid rectal cancer. LPLN metastasis occurs in approximately 10–25% of locally advanced rectal cancer patients and is a critical source of locoregional recurrence due to their location on the pelvic wall[5–8].

The management of LPLN metastasis in rectal cancer varies significantly between Eastern and Western countries[9]. In Eastern countries, particularly Japan, LPLN metastasis is treated as a locoregional spread, with the standard approach being TME combined with prophylactic LPLN dissection (LPLND) to reduce locoregional recurrence rates[10]. Conversely, in Western countries, LPLN metastasis is considered advanced disease, treated with neoadjuvant chemoradiotherapy (nCRT) followed by TME alone[11,12]. The technical challenges of LPLND and increased risk of postoperative complications contribute to this difference[13]. However, recent studies suggest that nCRT with TME alone is insufficient to prevent lateral local recurrence in patients with enlarged LPLNs[14]. Accurate preoperative prediction of LPLN metastasis is crucial to identify candidates who may benefit from LPLND.

Imaging modalities play a crucial role in the preoperative evaluation of LPLN metastasis. Among these, MRI is the primary tool for assessing primary tumors and perirectal lymph nodes, including LPLNs[15,16]. However, MRI has relatively low sensitivity and specificity in detecting LN metastases. Traditional MRI criteria, such as short-axis diameter and morphological features, have proven inadequate for reliable LPLN assessment[17,18], especially in patients treated with nCRT[19].

Radiomics, which involves extracting high-dimensional quantitative features from medical images, has emerged as a promising tool to address these limitations[20]. Radiomics has shown potential in enhancing the understanding of tumor behavior and improving patient management. This approach aligns with personalized medicine principles and has gained significant attention in radiology[21,22]. While numerous studies have applied radiomics to evaluate rectal cancer, focusing on primary tumors and perirectal lymph nodes[23,24], the application of MRI radiomics to predict LPLN metastasis remains underexplored.

This study aims to develop and validate an MRI radiomics-based prediction model for LPLN metastasis in rectal cancer patients who have undergone LPLND. Additionally, we aim to compare the performance of this radiomics model with that of radiologists using conventional size- and morphology-based criteria.

Materials and methods

This multicenter study was approved by the Institutional Review Board of three centers. The requirement for informed consent was waived due to the retrospective study design. All methods were performed in accordance with the relevant guidelines and regulations.

Patients

A search of the surgical database of three institutions revealed 491 patients who underwent rectal cancer surgery, including LPLND, between 2007 and 2020 (Fig. 1). Inclusion criteria were: (1) patients who underwent surgery including LPLND for rectal cancer with or without nCRT; (2) patients with post-nCRT, preoperative rectal MRI, if they had nCRT; (3) patients with preoperative rectal MRI, if they did not undergo nCRT; and (4) patients with pathologically proven adenocarcinoma. According to the inclusion criteria, 460 patients were eligible for enrollment. Exclusion criteria were: (1) > 2 month-interval between surgery and preoperative MRI ($n = 93$); (2) no available axial or oblique axial, coronal, and sagittal T2-weighted images ($n = 17$); and (3) poor image quality ($n = 14$). Finally, 336 patients constituted the study population. Among them, 190 patients from institutions 1 and 2 were allocated to the development cohort (DC), and 146 patients from institution 3 were allocated to the validation cohort (VC). Clinical and pathological information were obtained from electronic medical records.

Neoadjuvant chemoradiation therapy

Neoadjuvant therapy was performed in 266 patients (65/108 patients [60.2%] in institution 1, 58/82 in institution 2 [70.7%], and 143/146 patients in institution 3 [97.9%]). Detailed nCRT regimens are provided in Supplementary Material.

MR image acquisition

Post-nCRT, preoperative rectal MRI in 266 patients (123 patients in DC and 143 patients in VC) who underwent nCRT and preoperative MRI in 70 patients (67 in DC and 3 in VC) who underwent upfront surgery were used for analyses. All MRI examinations were performed with 1.5T or 3T MR scanners (Supplementary Table E1) and a 16-channel torso coil according to standard rectal MRI acquisition protocols. Rectal MRI included T2-weighted fast spin-echo sequences (Supplementary Table E2) in the sagittal, oblique axial, and oblique coronal planes, axial T1-weighted spin-echo sequences, diffusion-weighted images, and apparent diffusion coefficient maps. All T2-weighted images were saved as Digital Imaging and Communications in Medicine files.

MR image preprocessing and harmonization

Image preprocessing was performed to compare features from different MRI datasets. Steps included image interpolation, bias field correction, image normalization, and discretization. To produce MRI data with isotropic voxels ($1.0 \times 1.0 \times 1.0$ mm^3, a trilinear interpolation which uses the intensities of the eight nearby voxels in the original grid to calculate a new intensity was performed in 3-dimensional calculations[25] N4 bias field correction algorithm was applied to correct inhomogeneity of images, using the Nipype (Neuroimaging in Python: Pipelines and Interfaces) Python package (version 1.1.7; http://nipy.org/nipype)[26]. MR signal intensity normalization was

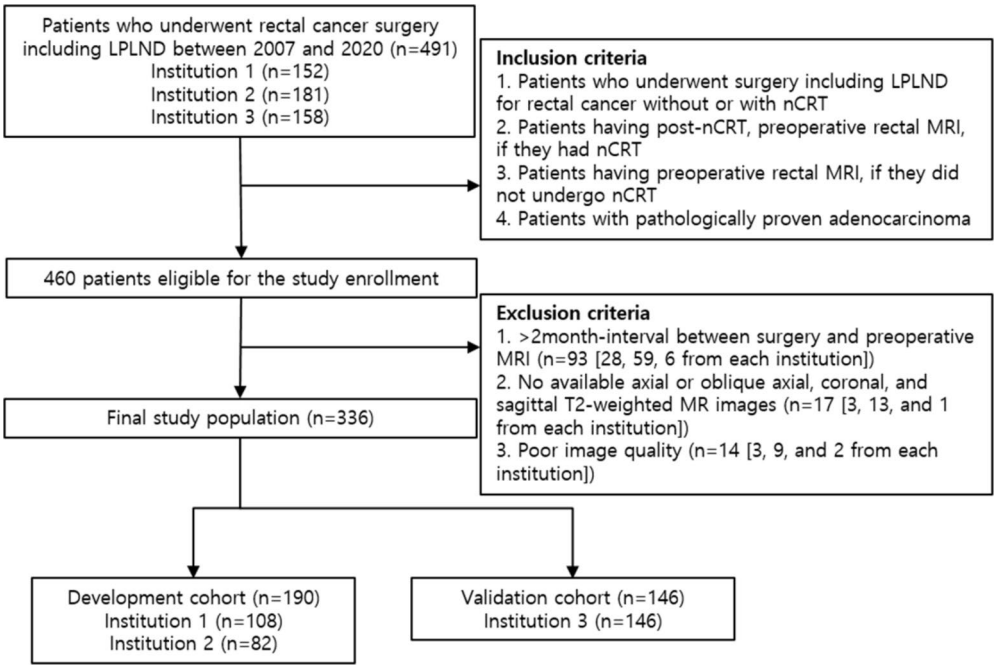

Fig. 1. A flow chart of patient enrollment. A total of 336 patients from 3 institutions were included in this study. Of these, 190 patients from institutions 1 and 2 were designated into the development cohort, and 146 patients from institution 3 were assigned to the validation cohort. *LPLND* lateral pelvic lymph node dissection, *nCRT* neoadjuvant chemoradiotherapy.

performed using PyRadiomics according to IBSI guidelines (https://ibsi.readthedocs.io/en/latest/index.html). Relative discretization using a fixed bin number of 128 was performed to reduce image noise. After radiomics feature extraction, harmonization was performed to reduce "center effect" noise due to technical differences in the images between centers using the R package neuroCombat (https://github.com/Jfortin1/neuroCombat_Rpackage) (Supplementary Material).

Semi-automated segmentation of LPLNs

After uploading T2-weighted MRI to commercially available segmentation and radiomics analysis software (MEDIP pro version 2.3.1, MEDICAL IP Co. Ltd., Seoul, Korea), semi-automated segmentation of LPLNs was conducted by a board-certified radiologist (J.Y with 9 years' experience in rectal MRI). All segmentation masks were confirmed by a senior radiologist (S.H.K with 24 years' experience). Both radiologists were blinded to clinicopathologic data. In patients with pathologically confirmed LPLN metastasis, the reported metastatic LN was matched with an LPLN on MRI using location and size from the pathologic report. In patients with no metastatic LN reported on surgical pathology, an LPLN showing the highest malignancy was selected. The imaging criteria suggesting metastatic LPLN were (1) short-axis diameter > 5 mm, (2) heterogeneous signal intensity, and (3) ill-defined or spiculated margin[27] When the radiologist placed a digital brush tool on the selected LN, an interactively controlled, growing color-overlay region of interest (ROI) was automatically displayed. Approximately 1 min per patient was needed for segmentation (Fig. 2).

Radiomics feature extraction, selection, and model construction

A total of 107 radiomics features were extracted from each ROI using the same software, according to PyRadiomics documentation (https://pyradiomics.readthedocs.io)[28] (Supplementary Material). The least absolute shrinkage and selection operator with nested cross-validation was used to select the optimal combination of predictive radiomics features for LPLN metastasis in the DC (Supplementary Material). Similarly, a clinical-radiomics model was constructed by combining the radiomics score and predictive clinical features. The R package nestedcv was used for model construction (version 4.2.1; R Foundation for Statistical Computing).

Radiologists' review

Two board-certified radiologists (HBY and KJH, with 16 years and 10 years of experience, respectively) independently reviewed T2-weighted MR images for 100 patients in the VC. The radiologists were aware that MRI was taken initially or after completion of nCRT, but blinded to histopathologic results. They selected an LPLN showing the highest malignant probability and rated the possibility of malignancy of LPLN using a 5-point confidence scale: 1, definitely benign; 2, probably benign; 3, possibly malignant; 4, probably malignant; 5, definitely malignant. For determining the malignant probability, the aforementioned criteria for metastatic LPLN were used. LPLNs meeting all three criteria were given a score of 5, whereas those meeting two or one criteria were given scores of 4 or 3, respectively. The location of each selected node was documented. After the

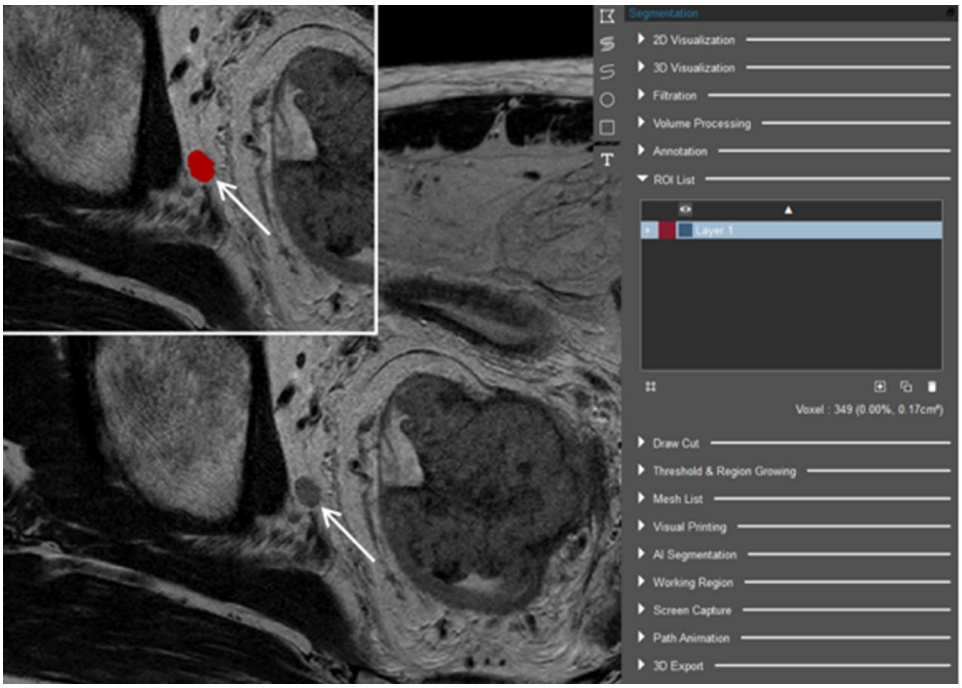

Fig. 2. Semi-automatic segmentation for lateral pelvic lymph node (LPLN) using a radiomics platform (MEDIP pro Version 2.3.1, MEDICAL IP Co. Ltd., Seoul, Korea). When the radiologist placed a digital brush tool on the selected lymph node (LN), an interactively controlled, growing color-overlay region of interest (ROI) was automatically displayed. If color-overlay ROIs extended outside the LPLN, an eraser tool was used to edit the contour and subtract the tissue volume. In this patient, an LPLN at the right internal iliac chain (arrow) was segmented and overlaid with red color.

first interpretation session, a second interpretation session was held for each radiologist with knowledge of the radiomics score with at least a 2-week interval to minimize recall bias.

Statistical analyses

Patient characteristics were compared between two cohorts using the Chi-square or Fisher's exact test for categorical variables and Mann-Whitney tests or t-tests for continuous variables. The diagnostic performance of each prediction model was assessed internally using 5-fold cross-validation. Discrimination was assessed by calculating the area under the curve (AUC) of the receiver operating characteristics (ROC) curve. ROC curve analysis was performed to compare performances between models and between models and radiologists. Additionally, comparative ROC analysis was done between radiologists without and with knowledge of the radiomics probability score. Calibration was assessed using a calibration plot. Decision curve analysis was conducted to evaluate the clinical utility of each predictive model by comparing the net benefits across a series of threshold probabilities. All statistical analyses were performed using R (version 4.2.1) and SAS software (version 9.4; SAS Institute).

Results

Demographics and clinical features

The positive rate for malignant LPLN was not significantly different between DC (34.2%, 65/190) and VC (32.9%, 48/146) ($P = 0.798$) (Table 1). However, neoadjuvant chemotherapy (64.2% [122/190] vs. 97.3% [142/146], $P < 0.001$) and neoadjuvant radiotherapy (62.6% [119/190] vs. 97.3% [142/146], $P < 0.001$) were more frequently performed in VC compared to DC. Additionally, the mean number of harvested mesorectal LN was significantly larger in DC (21 vs. 16, $P < 0.001$).

In the DC, patients with metastatic LPLNs showed significantly higher initial CEA levels, lower rates of nCRT, higher frequency of pathologic staging T3, higher pathologic N stage, lower rates of pathologically confirmed complete regression, and more frequent circumferential resection margin involvement by the tumor compared to those without metastatic LPLNs ($P < 0.05$) (Table 2).

Feature extraction and model construction

Among a total of 107 radiomics features, 6 were selected for the MR radiomics model: inverse variance, coarseness, elongation, maximal correlation coefficient, dependence entropy, and large dependence high gray level emphasis. For constructing a clinical-radiomics model, sex and neoadjuvant radiotherapy from clinical features and complexity from radiomics features were added to the six aforementioned radiomics features. The following equations were calculated for predicting metastatic LPLN.

Characteristics	Development cohort ($n = 190$)	Validation cohort ($n = 146$)	P value
Sex			0.823
Male	114 (60.0%)	85 (58.2%)	
Female	76 (40.0%)	61 (41.8%)	
Age (years), mean ± SD (range)	58.7 ± 11.3 (31–88)	59.0 ± 10.9 (30–83)	0.739
Initial CEA (ng/mL)*	20.0 ± 61.3 (0.4–610.0)	21.5 ± 69.7 (0.8–703.7)	0.259
Initial CA 19 – 9 (U/mL)†	110.8 ± 488.1 (0.9–4490.0)	45.3 ± 275.4 (0.9–3230.0)	0.065
Neoadjuvant chemotherapy			**< 0.001**
Yes	122 (64.2%)	142 (97.3%)	
No	68 (35.8%)	4 (2.7%)	
Neoadjuvant radiotherapy			**< 0.001**
Yes	119 (62.6%)	142 (97.3%)	
No	71 (37.4%)	4 (2.7%)	
Type of surgery			**< 0.001**
LAR	90 (47.4%)	77 (52.7%)	
ULAR	54 (28.4%)	11 (7.5%)	
APR	40 (21.1%)	16 (11.0%)	
ISR	6 (3.2%)	18 (12.3%)	
Transanal TME	0	22 (15.1%)	
Others	0	2 (1.4%)‡	
LPLN dissection			0.128
Unilateral	137 (72.1%)	116 (79.5%)	
Bilateral	53 (27.9%)	30 (20.5%)	
Metastatic LPLNs			0.445
Presence	65 (34.2%)	48 (32.9%)	
Absence	125 (65.8%)	98 (67.1%)	
No. of total metastatic LPLNs	0.8 ± 2.1 (0–19)	0.6 ± 1.2 (0–7)	0.521
T staging			0.429
Tis or no residual tumor	17 (8.9%)	10 (6.8%)	
T1	7 (3.7%)	5 (3.4%)	
T2	27 (14.2%)	31 (21.2%)	
T3	121 (63.7%)	83 (56.8%)	
T4	18 (9.5%)	17 (11.6%)	
N staging			0.366
N0	79 (41.6%)	72 (49.3%)	
N1	68 (35.8%)	46 (31.5%)	
N2	43 (22.6%)	28 (19.5%)	
Histopathologic type			0.480
Well differentiated	7 (3.7%)	11 (7.5%)	
Moderately differentiated	146 (76.8%)	116 (79.5%)	
Poorly differentiated	11 (5.8%)	5 (3.4%)	
Mucinous	9 (4.7%)	5 (3.4%)	
Signet ring cell	4 (2.1%)	2 (1.4%)	
N/A (no residual primary tumor)	13 (6.8%)	7 (4.8%)§	
Pathologically confirmed complete regression			0.203
Yes	13 (6.8%)	6 (4.1%)§	
No	177 (93.2%)	140 (95.9%)	
Resection margin			0.398
Clear	158 (83.2%)	116 (79.5%)	
Involved by tumor (< 1 mm)	32 (16.8%)	30 (20.5%)	
Circumferential margin involved	27 (14.2%)	28 (19.2%)	
Distal margin involved	4 (2.1%)	2 (1.4%)	
Both circumferential and distal margins involved	1 (0.5%)	0	
Tumor regression grade (AJCC)		NA	NA

Continued

Characteristics	Development cohort ($n=190$)	Validation cohort ($n=146$)	P value
0 (no viable cancer cell)	16 (8.4%)		
1 (moderate response)	27 (14.2%)		
2 (minimal response)	62 (32.6%)		
3 (poor response)	18 (9.5%)		
N/A (no neoadjuvant treatment)	67 (35.3%)		
Tumor regression grade (Dworak)	NA		NA
0 (no response)		8 (5.5%)	
1 (minimal response)		44 (30.1%)	
2 (moderate response)		77 (52.7%)	
3 (near complete response)		11 (7.5%)	
4 (complete response, no tumor cells)		6 (4.1%)	

Table 1. Characteristics of development and validation cohorts. *SD* standard deviation, *CEA* carcinoembryonic antigen, *CA19-9* carbohydrate antigen 19-9, *LAR* low anterior resection, *ULAR* ultra-low anterior resection, *APR* anterior perineal resection, *ISR* inter-sphincteric resection, *TME* total mesorectal excision, *LPLN* lateral pelvic lymph node, *N/A* not applicable, *AJCC* American Joint Committee on Cancer. *Data were available in 181 patients from the development cohort and 144 from the validation cohort. †Data were available in 113 patients from the development cohort and 142 from the validation cohort. ‡Subtotal proctocolectomy was performed in two patients. §Complete regression of primary tumor and regional lymph nodes was pathologically confirmed in six patients, and complete regression of primary tumor with residual metastatic regional lymph nodes was confirmed in one patient. Significant values are in bold.

$$\begin{aligned} Radiomics\ probability\ score = &-3.129 + (17.75 \times inverse\ variance) - (11.79 \times coarseness) + (1.349 \times elongation) \\ &- (1.249 \times maximal\ correlation\ coefficient) + (0.3133 \times dependence\ entropy) \\ &+ (0.00002075 \times large\ dependence\ high\ gray\ level\ emphasis) \end{aligned}$$

$$\begin{aligned} Clinical-radiomics\ probability\ score = &-3.6169 + (17.57 \times inverse\ variance) - (14.06 \times coarseness) + (1.638 \times elongation) \\ &- (0.8323 \times maximal\ correlation\ coefficient) + (0.4421 \times sex\ [female] \\ &+ (0.3008 \times dependence\ entropy) - (0.2747 \times neoadjuvant\ radiotherapy\ [yes]) \\ &+ (0.00002171 \times large\ dependence\ high\ gray\ level\ emphasis) + (0.0000006628 \times complexity) \end{aligned}$$

Comparison of model performance

The radiomics model and clinical-radiomics model demonstrated AUCs of 0.819 (95% CI, 0.753–0.886) and 0.830 (95% CI, 0.767–0.893), respectively, in DC for predicting metastatic LPLN (Table 3). Five-fold cross-internal validation showed no significant difference in AUC values between the radiomics and clinical-radiomics models (0.772 [95% CI, 0.698–0.846] vs. 0.762 [95% CI, 0.686–0.837], $P=0.186$). External validation using the VC also demonstrated no significant difference in performance between the two models (0.821 [95% CI, 0.747–0.896] vs. 0.829 [95% CI, 0.756–0.901], $P=0.505$).

The optimal cut-off radiomics score for discriminating metastatic LPLN was determined to be − 0.47 using the Youden index. Based on this cut-off value, a radiomics score of ≥− 0.47 predicts metastatic LPLN. Sensitivity was 72.3% (95% CI, 61–83%) and specificity was 82.4% (95% CI, 76–89%) in DC, while sensitivity was 45.8% (95% CI, 32–60%) and specificity was 87.8% (95% CI, 81-94%) in VC.

The calibration curves of the two prediction models showed similar performance in both internal (Fig. 3a) and external validation (Fig. 3b). In internal validation, both models showed good calibration, but tended to slightly underestimate the risk of metastatic LPLN in external validation. Additionally, prediction accuracy was not improved when clinical features were added to the radiomics model, compared to the radiomics model alone in both internal and external validation.

Decision curve analysis demonstrated that the clinical-radiomics model provided no additional net benefit compared to the radiomics model alone for predicting LPLN metastasis in both internal (Fig. 4a) and external validation (Fig. 4b).

Radiologists' discriminative performance

In a subset of VC ($n=100$), the rate of metastatic LPLN was 31.0% (31/100). Additionally, most patients (97%, 97/100) received nCRT. The AUC of the radiomics model (0.842) was significantly higher than those of both radiologists (0.734 and 0.668, respectively) ($P<0.05$) (Table 4). AUC values of both radiologists significantly increased when radiomics probability scores were provided (from 0.734 to 0.801 for radiologist 1, $P=0.037$; from 0.668 to 0.791 for radiologist 2, $P=0.047$) (Fig. 5). Representative cases are shown in Fig. 6.

Discussions

In this study, we demonstrate that the radiomics model, both alone and in combination with clinical features, significantly improves the accuracy of predicting LPLN metastasis compared to traditional size- and morphology-based criteria used by radiologists. Our findings indicate that the radiomics model achieved good discriminative performance, with AUCs of 0.819 in DC and 0.821 in the external VC. The model's sensitivity and specificity

	Patients without metastatic LPLN ($n = 125$)	Patients with metastatic LPLN ($n = 65$)	*P*-value
Sex			0.061
Male	81 (64.8%)	33 (50.8%)	
Female	44 (35.2%)	32 (49.2%)	
Age (mean ± SD)	59.3 ± 11.9 years	57.6 ± 10.0 years	0.319
Initial CEA (mean ± SD)	10.2 ± 22.6 ng/mL	31.3 ± 85.6 ng/mL	**0.007**
Preoperative CEA (mean ± SD)	2.0 ± 1.6 ng/mL	2.1 ± 2.1 ng/mL	0.942
Neoadjuvant chemotherapy			**0.005**
Yes	89 (71.2%)	33 (50.8%)	
No	36 (28.8%)	32 (49.2%)	
Neoadjuvant radiotherapy			**0.002**
Yes	88 (70.4%)	31 (47.7%)	
No	37 (29.6%)	34 (52.3%)	
T staging			**0.005**
Tis or no residual tumor	16 (12.8%)	1 (1.5%)	
T1	3 (2.4%)	4 (6.2%)	
T2	23 (18.4%)	4 (6.2%)	
T3	71 (56.8%)	50 (76.9%)	
T4	12 (9.6%)	6 (9.2%)	
N staging			**< 0.001**
N0	79 (63.2%)	0	
N1	35 (28.0%)	33 (50.8%)	
N2	11 (8.8%)	32 (49.2%)	
Tumor regression grade (AJCC)			0.055
0 (no viable cancer cell)	16 (12.8%)	0	
1 (moderate response)	17 (13.6%)	9 (13.8%)	
2 (minimal response)	42 (33.6%)	19 (29.2%)	
3 (poor response)	14 (11.2%)	4 (6.2%)	
N/A (no neoadjuvant treatment)	4 (3.2%)	33 (50.8%)	
Pathologically confirmed CR			**0.005**
Yes	13 (10.4%)	0	
No	112 (89.6%)	65 (100.0%)	
Resection margin			0.053
Clear	114 (91.2%)	53 (81.5%)	
Involved by tumor (< 1 mm)	11 (8.8%)	12 (18.5%)	
Circumferential resection margin			**0.006**
Clear	113 (90.4%)	49 (75.4%)	
Involved by tumor (< 1 mm)	12 (9.6%)	16 (24.6%)	
Distal resection margin			1.000
Clear	122 (97.6%)	63 (96.9%)	
Involved by tumor (< 1 mm)	3 (2.4%)	2 (3.1%)	
Histopathologic type			0.908
Well differentiated	5 (4.0%)	2 (3.1%)	
Moderately differentiated	94 (75.2%)	52 (80.0%)	
Poorly differentiated	6 (4.8%)	5 (7.7%)	
Mucinous	5 (4.0%)	4 (6.2%)	
Signet ring cell	2 (1.6%)	2 (3.1%)	
N/A (no residual primary tumor)	13 (10.4%)	0	

Table 2. Comparison of clinical and pathologic features between patients with and without metastatic LPLNs in the development cohort. *LPLN* lateral pelvic lymph node, *SD* standard deviation, *CEA* carcinoembryonic antigen, *AJCC* American Joint Committee on Cancer, *N/A* not applicable, *CR* complete remission. Significant values are in bold.

suggest it is a robust tool for identifying metastatic LPLNs. Notably, the inclusion of clinical features (sex and neoadjuvant radiotherapy) did not significantly enhance the model's performance, highlighting the substantial predictive power of radiomics model alone. Furthermore, the calibration curve for both models show good calibration performance in both internal and external validations, indicating that the predictions align closely

	Development cohort	Internal validation*		External validation	
	AUC (95% CI)	AUC (95% CI)	P value	AUC (95% CI)	P value
Radiomics model†	0.819 (0.753–0.886)	0.772 (0.698–0.846)	0.186	0.821 (0.747–0.896)	0.505
Clinical-radiomics model‡	0.830 (0.767–0.893)	0.762 (0.686–0.837)		0.829 (0.756–0.901)	

Table 3. Comparison of diagnostic performances between radiomics model and combined clinical-radiomics model. *AUC* area under the curve, *CI* confidence interval. *Internal validation was performed using a fivefold cross validation. †Six selected radiomics features were inverse variance, coarseness, elongation, maximal correlation coefficient, dependence entropy, and large dependence high gray level emphasis. ‡Nine selected clinical-radiomics features were inverse variance, coarseness, elongation, maximal correlation coefficient, dependence entropy, large dependence high gray level emphasis, complexity, sex, and neoadjuvant radiotherapy.

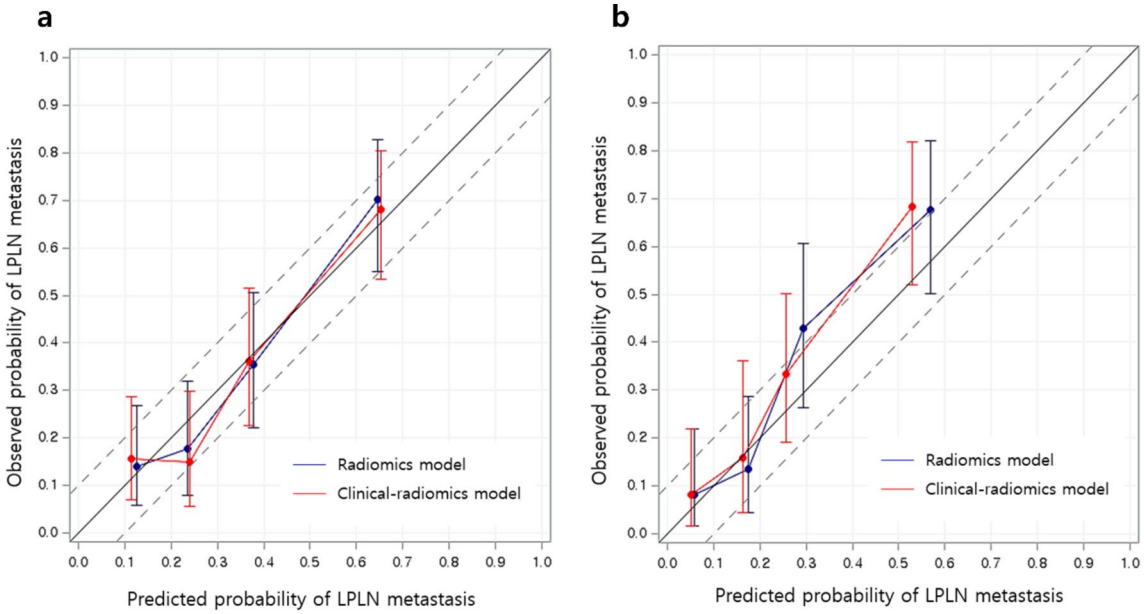

Fig. 3. Calibration curves of radiomics and clinical-radiomics models in 5-fold cross internal validation (**a**) and external validation (**b**). In the calibration curves of prediction models, no better prediction accuracy was achieved when clinical features were added to the radiomics model in both internal (**a**) and external validation (**b**).

with the actual observed probabilities. The similarity in calibration performance suggests that radiomics features are robust predictors of LPLN metastasis and that clinical features do not drastically enhance the model's predictive capability. This finding simplifies model integration into clinical workflows, reducing the need for extensive clinical data collection.

In our study, 7 out of 107 radiomics features were finally selected for the radiomics or clinical-radiomics model. Each of these radiomics features provides unique insights into the texture (inverse variance, coarseness, maximal correlation coefficient, and large dependence high gray level emphasis), shape (elongation), and structural (dependence entropy and complexity) characteristics of the LNs, enhancing the ability to distinguish between benign and metastatic nodes based on their imaging properties. Maximal correlation coefficient and large dependence high gray level emphasis measure the degree of dependency between neighboring pixels. A higher value could indicate a stronger correlation between neighboring pixel values, which might reflect chaotic structures of malignant nodes. In addition, two structural features measure the randomness and complexity in the spatial distribution of pixel intensities. Higher entropy and complexity suggest a more disordered and irregular texture, which could be characteristic of malignant LNs. These features capture subtle differences in tissue heterogeneity and structure that are not easily discernible through conventional imaging interpretation by radiologists.

Our results align with previous research indicating that MRI alone has limited sensitivity and specificity for determining LN metastasis and that MRI radiomics can significantly improve differentiation between benign and malignant LNs across various cancers, including breast, cervical, and endometrial cancer[29–31]. A recent meta-analysis also suggested that MR radiomics can predict LN metastasis more accurately in rectal cancer patients and outperform radiologists' performance[32]. However, no prior study focused on LPLN in rectal cancer MRI. Although Nakanishi et al. demonstrated the potential of radiomics for predicting LPLN metastasis using

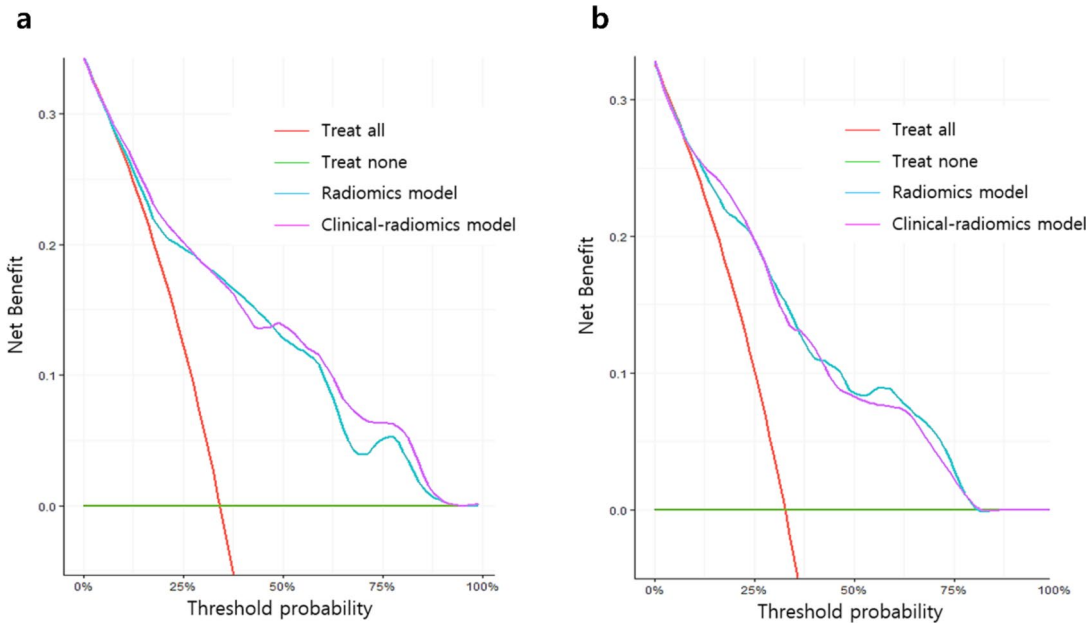

Fig. 4. Decision curve analysis. The decision curve analysis demonstrated that the clinical-radiomics model provided no additional net benefit over the radiomics-only model for predicting LPLN metastasis in both internal (**a**) and external validation (**b**).

	AUC (95% CI)	*P* value*
Radiomics model	0.842 (0.757–0.927)	Reference
Reviewer 1	0.734 (0.624–0.844)	0.015
Reviewer 2	0.668 (0.530–0.805)	0.010

Table 4. Comparison of diagnostic performances between the radiomics model and each radiologist and in a subset of validation cohort ($n = 100$). *AUC* area under the curve, *CI* confidence interval. *P values were calculated using radiomics model as a reference.

contrast-enhanced CT[33], our study is the first to apply radiomics to MRI for predicting LPLN metastasis in rectal cancer, expanding the potential applications of radiomics in oncologic imaging.

This study focused on comparing radiologists' performance to the radiomics model in predicting LPLN metastasis. In a VC subset ($n = 100$), the radiomics model showed a superior AUC of 0.842, outperforming radiologists' AUCs of 0.734 and 0.668. This suggests that the radiomics model has a higher discriminative ability to identify metastatic LPLNs compared to traditional methods used by radiologists. Because most (97/100, 97%) patients in this subset of the VC received nCRT, determining metastatic LN might be more challenging for human readers compared to naïve patients. Conversely, the radiomics model's ability to analyze high-dimensional data and extract subtle MRI features provides a more comprehensive assessment than human interpretation alone. When radiologists used radiomics probability scores as a second opinion, their AUCs improved significantly. This demonstrates radiomics' potential to enhance radiological assessments and improve LPLN metastasis prediction.

The integration of radiomics probability scores into radiologists' workflows has several important clinical implications. First, combining radiomics and expert interpretation can lead to more accurate identification of metastatic LPLNs, critical for optimal treatment planning in rectal cancer patients. Accurate discrimination of LPLN allows for better stratification of patients for LPLN dissection versus those managed with nCRT alone, preventing unnecessary and futile LPLN dissection. This tailored approach can potentially improve patient outcomes by ensuring that those at higher risk of metastasis receive the most appropriate treatment. Second, radiomics provides an objective, reproducible, and quantitative assessment, reducing inter-reader variability and leading to more consistent diagnoses and treatment decisions. Additionally, radiomics probability scores can educate radiologists, helping them identify imaging features indicative of metastasis, thereby enhancing their interpretive skills and diagnostic confidence over time.

Several limitations of our study should be acknowledged. First, the retrospective design and relatively small sample size may limit the generalizability of our findings. Future studies should include larger, multicenter cohorts to validate our results across diverse populations. Second, the MRI acquisition protocols varied across institutions, which, despite harmonization efforts, may introduce variability in feature extraction. Standardizing imaging protocols could enhance the robustness of radiomics models. Additionally, while our model performed

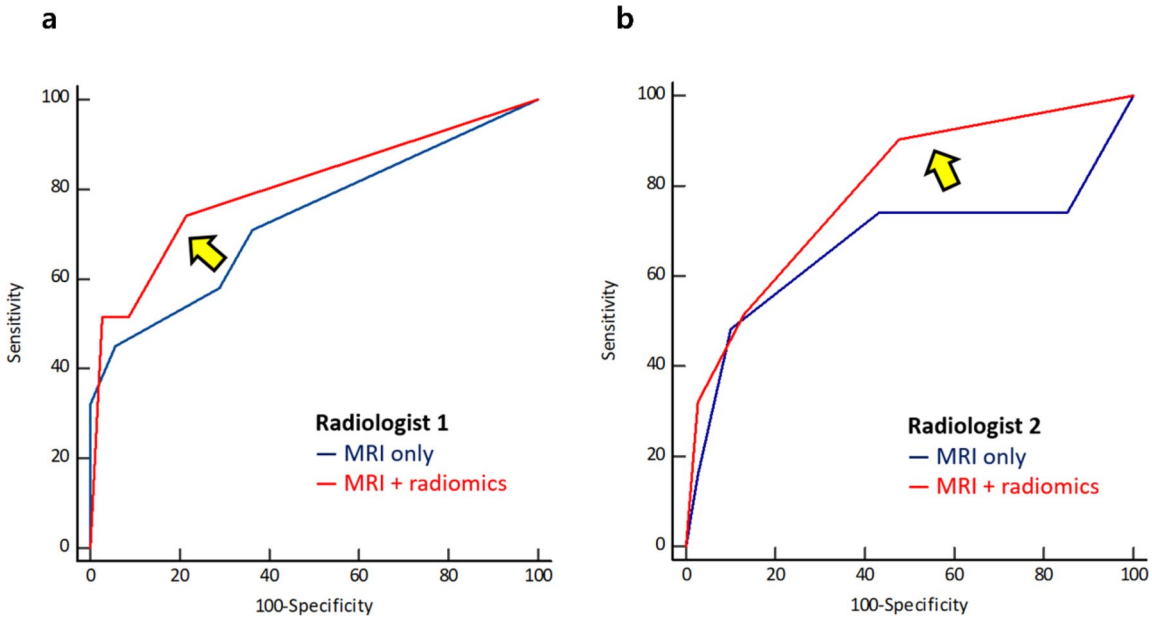

Fig. 5. Receiver operating characteristic curves of both radiologists without and with knowledge of the radiomics probability score for predicting lateral pelvic lymph node metastasis. The area under the curve values for both radiologists significantly increased when the radiomics probability score was provided (from 0.734 to 0.801 for radiologist 1 (**a**), $P = 0.047$; from 0.668 to 0.791 for radiologist 2 (**b**), $P = 0.037$).

well in the external VC, its sensitivity was lower compared to the DC. This discrepancy underscores the need for continuous refinement and validation of radiomics models in different clinical settings. Finally, we did not include diffusion-weighted imaging (DWI) which is a valuable MR sequence in the evaluation of LNs in rectal cancer. However, in the context of rectal cancer patients who have frequently undergone nCRT, LNs often become significantly smaller and may demonstrate reduced conspicuity on DWI. This poses challenges for reliable and reproducible segmentation, which is critical for radiomics analysis. The lower spatial resolution and increased susceptibility to distortion artifacts in DWI further complicate accurate delineation of small LNs post-treatment. Therefore, in this study, we focused on T2-weighted images, which offer higher anatomical detail and allow more consistent segmentation of LNs, particularly in the post-nCRT setting. Nonetheless, we believe that incorporating DWI into future radiomics analyses holds great promise and further studies that integrate both T2-weighted images and DWI should be performed to improve diagnostic performance for characterizing lateral pelvic LNs in rectal cancer patients.

Future research should focus on prospective studies to confirm the clinical utility of the radiomics model in routine rectal MRI practice. Integrating radiomics with other modalities, such as PET/CT, or incorporating genomic data could improve predictive accuracy and provide a more comprehensive understanding of metastatic pathways. Moreover, developing user-friendly software tools that can seamlessly integrate radiomics analysis into existing PACS systems will be crucial for practical application. Collaborative efforts between radiologists, oncologists, and data scientists will be essential to advance the field and translate radiomics research into tangible clinical benefits.

In conclusion, a radiomics approach using MRI images can effectively predict LPLN metastasis in rectal cancer patients, improving traditional size- and morphology-based criteria. It holds promise for enhancing diagnostic accuracy and guiding treatment strategies.

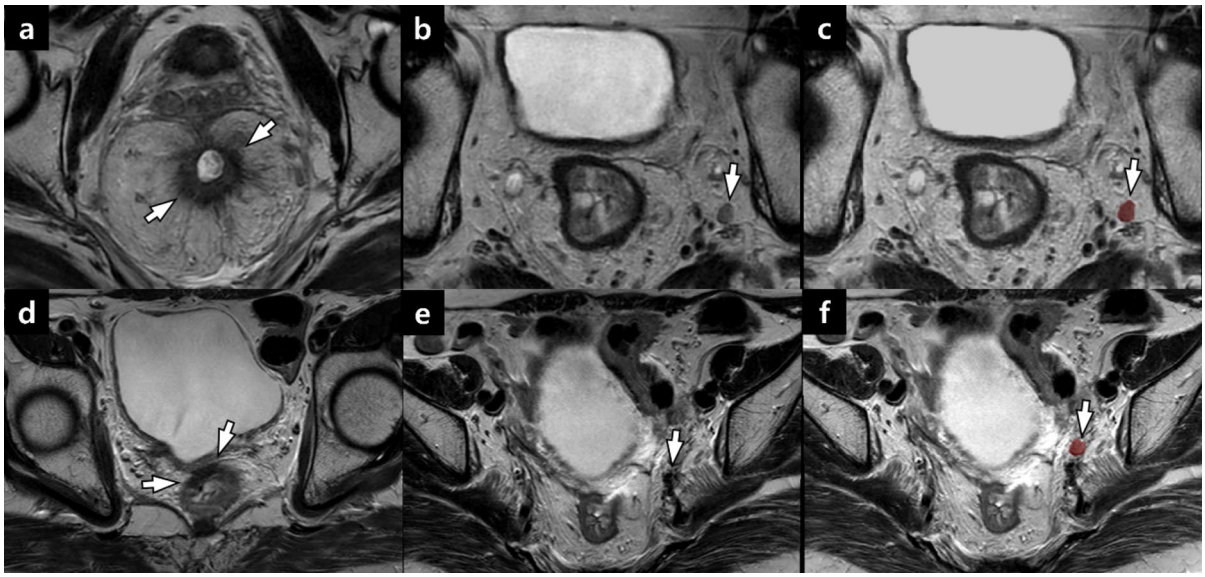

Fig. 6. A 66-year-old man who underwent neoadjuvant chemoradiotherapy for rectal cancer. (**a**) Axial T2-weighted image demonstrates a circumferential wall thickening of the rectum (arrows), suggesting rectal cancer. **(b)** On an axial T2-weighted image, a 6 mm lymph node (LN) in short axis (arrow) with a well-defined margin and homogeneous signal intensity is seen at the left internal iliac chain. Both reviewers assigned a score of 3 (indeterminate) to this LN. **(c)** On a radiomics platform, the LN was semi-automatically segmented (arrow). According to the radiomics-based model, the calculated score was − 0.37, higher than the cutoff of − 0.47. The reviewers revised their scores from 3 to 4 (probably malignant) in the second interpretation session, considering the radiomics score. The patient underwent low anterior resection with bilateral lateral pelvic LN dissection, and the left internal iliac LN was pathologically confirmed as metastatic. The final pathologic staging was ypT3bN1. A 73-year-old woman who underwent neoadjuvant chemoradiotherapy for rectal cancer. **(d)** T2-weighted axial image shows a focal eccentric wall thickening with low signal intensity in the rectum (arrows), suggesting rectal cancer after neoadjuvant therapy. **(e)** On an axial T2-weighted image, a 6 mm LN in short axis (arrow) with homogeneous signal intensity and a well-defined margin is seen at the left internal iliac chain. Both reviewers assigned a score of 3 (indeterminate) to this LN. **(f)** On a radiomics platform, the LN was semi-automatically segmented (arrow). The radiomics score of this LN was − 3.09, below the cutoff of − 0.47. The reviewers revised the scores from 3 to 1 (definitely benign) in the second interpretation session, considering the radiomics score. The patient underwent low anterior resection with bilateral lateral pelvic LN dissection, and the left internal iliac LN was pathologically confirmed as benign. The final pathologic staging was ypT0N0.

Data availability

The datasets used and/or analysed during the current study are available from the corresponding author on reasonable request.

Received: 23 December 2024; Accepted: 16 April 2025
Published online: 29 April 2025

References

1. Bray, F. et al. Global cancer statistics 2018: GLOBOCAN estimates of incidence and mortality worldwide for 36 cancers in 185 countries. *CA Cancer J. Clin.* **68**, 394–424. https://doi.org/10.3322/caac.21492 (2018).
2. Heald, R. J., Husband, E. M. & Ryall, R. D. The mesorectum in rectal cancer surgery–the clue to pelvic recurrence? *Br. J. Surg.* **69**, 613–616. https://doi.org/10.1002/bjs.1800691019 (1982).
3. Knol, J. & Keller, D. S. Total mesorectal excision technique-past, present, and future. *Clin. Colon Rectal Surg.* **33**, 134–143. https://doi.org/10.1055/s-0039-3402776 (2020).
4. Maurer, C. A. et al. The impact of the introduction of total mesorectal excision on local recurrence rate and survival in rectal cancer: long-term results. *Ann. Surg. Oncol.* **18**, 1899–1906. https://doi.org/10.1245/s10434-011-1571-0 (2011).
5. Christou, N., Meyer, J., Toso, C., Ris, F. & Buchs, N. C. Lateral lymph node dissection for low rectal cancer: is it necessary? *World J. Gastroenterol.* **25**, 4294–4299. https://doi.org/10.3748/wjg.v25.i31.4294 (2019).
6. Kim, T. H. et al. Lateral lymph node metastasis is a major cause of locoregional recurrence in rectal cancer treated with preoperative chemoradiotherapy and curative resection. *Ann. Surg. Oncol.* **15**, 729–737. https://doi.org/10.1245/s10434-007-9696-x (2008).
7. Atef, Y. et al. Lateral pelvic lymph node metastases in rectal cancer: a systematic review. *World J. Surg.* **43**, 3198–3206. https://doi.org/10.1007/s00268-019-05135-3 (2019).
8. Akiyoshi, T. et al. Results of a Japanese nationwide multi-institutional study on lateral pelvic lymph node metastasis in low rectal cancer: is it regional or distant disease? *Ann. Surg.* **255**, 1129–1134. https://doi.org/10.1097/SLA.0b013e3182565d9d (2012).
9. Kusters, M., Uehara, K., Velde, C. & Moriya, Y. Is there any reason to still consider lateral lymph node dissection in rectal cancer? Rationale and technique. *Clin. Colon Rectal Surg.* **30**, 346–356. https://doi.org/10.1055/s-0037-1606112 (2017).

10. Hashiguchi, Y. et al. Japanese society for Cancer of the Colon and rectum (JSCCR) guidelines 2019 for the treatment of colorectal cancer. *Int. J. Clin. Oncol.* **25**, 1–42. https://doi.org/10.1007/s10147-019-01485-z (2020).
11. van de Velde, C. J. et al. EURECCA colorectal: multidisciplinary management: European consensus conference colon & rectum. *Eur. J. Cancer* **50**, e1–e34. https://doi.org/10.1016/j.ejca.2013.06.048 (2014).
12. Schmoll, H. J. et al. ESMO consensus guidelines for management of patients with colon and rectal cancer. A personalized approach to clinical decision making. *Ann. Oncol.* **23**, 2479–2516. https://doi.org/10.1093/annonc/mds236 (2012).
13. Yano, H. & Moran, B. J. The incidence of lateral pelvic side-wall nodal involvement in low rectal cancer May be similar in Japan and the West. *Br. J. Surg.* **95**, 33–49. https://doi.org/10.1002/bjs.6061 (2008).
14. Ogura, A. et al. Neoadjuvant (chemo)radiotherapy with total mesorectal excision only is not sufficient to prevent lateral local recurrence in enlarged nodes: results of the multicenter lateral node study of patients with low cT3/4 rectal cancer. *J. Clin. Oncol.* **37**, 33–43. https://doi.org/10.1200/jco.18.00032 (2019).
15. Ogawa, S. et al. Selection of lymph node-positive cases based on perirectal and lateral pelvic lymph nodes using magnetic resonance imaging: study of the Japanese society for Cancer of the Colon and rectum. *Ann. Surg. Oncol.* **23**, 1187–1194. https://doi.org/10.1245/s10434-015-5021-2 (2016).
16. Sekido, Y. et al. Predicting lateral pelvic lymph node metastasis based on magnetic resonance imaging before and after neoadjuvant chemotherapy for patients with locally advanced lower rectal cancer. *Surg. Today.* **50**, 292–297. https://doi.org/10.1007/s00595-019-01886-7 (2020).
17. Li, X. T., Sun, Y. S., Tang, L., Cao, K. & Zhang, X. Y. Evaluating local lymph node metastasis with magnetic resonance imaging, endoluminal ultrasound and computed tomography in rectal cancer: a meta-analysis. *Colorectal Dis.* **17**, O129–135. https://doi.org/10.1111/codi.12909 (2015).
18. Zhuang, Z., Zhang, Y., Wei, M., Yang, X. & Wang, Z. Magnetic resonance imaging evaluation of the accuracy of various lymph node staging criteria in rectal cancer: a systematic review and meta-analysis. *Front. Oncol.* **11**, 709070. https://doi.org/10.3389/fonc.2021.709070 (2021).
19. Akiyoshi, T. et al. Indications for lateral pelvic lymph node dissection based on magnetic resonance imaging before and after preoperative chemoradiotherapy in patients with advanced low-rectal cancer. *Ann. Surg. Oncol.* **22** (Suppl 3), 614–620. https://doi.org/10.1245/s10434-015-4565-5 (2015).
20. Kumar, V. et al. Radiomics: the process and the challenges. *Magn. Reson. Imaging.* **30**, 1234–1248. https://doi.org/10.1016/j.mri.2012.06.010 (2012).
21. Gillies, R. J., Kinahan, P. E. & Hricak, H. Radiomics: images are more than pictures, they are data. *Radiology* **278**, 563–577. https://doi.org/10.1148/radiol.2015151169 (2016).
22. Aerts, H. J. W. L. et al. Decoding tumour phenotype by noninvasive imaging using a quantitative radiomics approach. *Nat. Commun.* **5**, 4006. https://doi.org/10.1038/ncomms5006 (2014).
23. Li, M. et al. A clinical-radiomics nomogram for the preoperative prediction of lymph node metastasis in colorectal cancer. *J. Translational Med.* **18**, 46. https://doi.org/10.1186/s12967-020-02215-0 (2020).
24. Huang, Y. Q. et al. Development and validation of a radiomics nomogram for preoperative prediction of lymph node metastasis in colorectal cancer. *J. Clin. Oncol.* **34**, 2157–2164. https://doi.org/10.1200/jco.2015.65.9128 (2016).
25. Zwanenburg, A. et al. The image biomarker standardization initiative: standardized quantitative radiomics for high-throughput image-based phenotyping. *Radiology* **295**, 328–338 (2020).
26. Dovrou, A. et al. A segmentation-based method improving the performance of N4 bias field correction on T2weighted MR imaging data of the prostate. *Magn. Reson. Imaging.* **101**, 1–12. https://doi.org/10.1016/j.mri.2023.03.012 (2023).
27. Horvat, N., Rocha, C. T., Clemente Oliveira, C., Petkovska, B., Gollub, M. & I. & J. MRI of rectal cancer: tumor staging, imaging techniques, and management. *Radiographics* **39**, 367–387 (2019).
28. van Griethuysen, J. J. M. et al. Computational radiomics system to Decode the radiographic phenotype. *Cancer Res.* **77**, e104–e107. https://doi.org/10.1158/0008-5472.Can-17-0339 (2017).
29. Song, D. et al. Dynamic contrast-enhanced MRI radiomics nomogram for predicting axillary lymph node metastasis in breast cancer. *Cancer Imaging.* **22**, 17. https://doi.org/10.1186/s40644-022-00450-w (2022).
30. Wang, T., Li, Y. Y., Ma, N. N., Wang, P. A. & Zhang, B. A MRI radiomics-based model for prediction of pelvic lymph node metastasis in cervical cancer. *World J. Surg. Oncol.* **22**, 55. https://doi.org/10.1186/s12957-024-03333-5 (2024).
31. Di Donato, V. et al. Magnetic resonance imaging-radiomics in endometrial cancer: a systematic review and meta-analysis. *Int. J. Gynecol. Cancer.* **33**, 1070–1076. https://doi.org/10.1136/ijgc-2023-004313 (2023).
32. Bedrikovetski, S. et al. Artificial intelligence for pre-operative lymph node staging in colorectal cancer: a systematic review and meta-analysis. *BMC Cancer.* **21**, 1058. https://doi.org/10.1186/s12885-021-08773-w (2021).
33. Nakanishi, R. et al. Radiomics approach outperforms diameter criteria for predicting pathological lateral lymph node metastasis after neoadjuvant (chemo)radiotherapy in advanced low rectal cancer. *Ann. Surg. Oncol.* **27**, 4273–4283. https://doi.org/10.1245/s10434-020-08974-w (2020).

Author contributions

J Yoo: data interpretation and drafting of the manuscript; J Y Han: data collection and drafting of the manuscript; W Chang: data collection; B Y Hur: data collection; J H Kim: data collection; Y Choi: statistical analyses; S J Kim: data collection; S H Kim: conceptualization and supervision of the study, review and editing of the manuscript. All authors read and approved the final version of the manuscript.

Funding

This research was supported by Basic Science Research Program through the National Research Foundation of Korea [NRF] funded by the Ministry of Science, ICT& Future Planning (NRF-2021R1F1A1046393) and from the Seoul National University Hospital Research Fund No. 03-2023-0340.

Declarations

Competing interests

The authors declare no competing interests.

Ethical approval

This retrospective study was approved by institutional review boards of Seoul National University Hospital, Seoul National University Bundang Hospital, and National Cancer Center.

Additional information

Supplementary Information The online version contains supplementary material available at https://doi.org/10.1038/s41598-025-99029-1.

Correspondence and requests for materials should be addressed to S.H.K.

Reprints and permissions information is available at www.nature.com/reprints.

Publisher's note Springer Nature remains neutral with regard to jurisdictional claims in published maps and institutional affiliations.

Supplementary Information The online version contains supplementary material available at https://doi.org/10.1038/s41598-025-99029-1.